PHYSICAL REVIEW C **77**, 054603 (2008)

Pickup coupling effects in deuteron scattering: The case of $d + {}^{40}$Ca

N. Keeley[*,†]
CEA/DSM/IRFU/SPhN Saclay, F-91191 Gif-sur-Yvette Cedex, France

R. S. Mackintosh[‡]
Department of Physics and Astronomy, The Open University, Milton Keynes, MK7 6AA, United Kingdom
(Received 19 February 2008; published 15 May 2008)

The dynamic polarization potential (DPP) contribution to the effective deuteron-nucleus interaction is evaluated by means of coupled reaction channel (CRC) calculations followed by S-matrix-to-potential inversion. The full coupled channel S matrix $S^J_{l'l}$ is inverted using the iterative-perturbative algorithm to yield a potential that includes a complex T_R tensor term as well as central and spin-orbit components. The differences between the various components of the inverted potential and the corresponding terms in the bare potential of the CRC calculation constitute a local equivalent representation of the complete DPP that is generated by the reaction channel coupling. The magnitude of the DPP, the real part in particular, is much less than that found in earlier calculations in which the nonorthogonality terms were omitted. The characteristic features of the tensor part of the DPP were traced to breakup and reorientation processes in the entrance deuteron channel that had been included with the pickup. The contribution of stripping to the deuteron-nucleus interaction is also discussed.

DOI: 10.1103/PhysRevC.77.054603 PACS number(s): 25.45.−z, 24.10.−i, 24.50.+g, 24.70.+s

I. INTRODUCTION

It is now known that the coupling of pickup channels makes a substantial contribution to the nucleon-nucleus interaction (see, e.g., Ref. [1]). Reference [1] cites a sequence of papers covering nearly 35 years in which improvements in computing facilities and programming sophistication have successively allowed the inclusion of finite-range stripping interactions, as well as nonorthogonality and remnant terms in coupled reaction channel (CRC) calculations. Although these successive improvements have indeed led to a substantial reduction in the calculated effect of pickup (deuteron) channels on nucleon scattering, substantial modifications of both the real and imaginary components remain. That part of the nucleon-nucleus interaction that is due to pickup channel coupling has been determined by $S_{lj} \rightarrow V(r)$ inversion of the diagonal S matrix from the CRC calculation; it cannot be represented as a renormalization of the folding model potential.

It is natural to apply the same procedure to deuteron scattering and to ask what contribution to the deuteron optical potential is induced by the coupling of mass-3 channels. Earlier work [2] found surprisingly large contributions to the real and imaginary central components of the deuteron optical potential. However, that work was based on zero-range CRC calculations that omitted nonorthogonality contributions. The first major purpose of this work is to exploit the refinements that have now become possible in CRC calculations, with the advent of sophisticated codes such as FRESCO [3], to re-evaluate the contribution of pickup to the real and imaginary central components of the deuteron optical potential. In addition, it has now become possible [4] to invert the coupled channel S matrix for spin-1 projectiles to yield a potential that includes a tensor component; in this way one can explicitly determine the tensor as well as spin-orbit interactions that are generated by such reaction channel couplings. This is the second major purpose of the work described here: to explore the contribution of the coupling of mass-3 channels to the spin-dependent parts of the deuteron-nucleus interaction and the tensor interaction in particular. The investigations lead to a number of interesting general features concerning the complex and spin-dependent dynamical polarization potential (DPP) that are due to coupled reaction channels.

The present calculations are restricted to a single case, that of 52-MeV deuterons scattering from ^{40}Ca, for which both elastic scattering data and pickup reaction data exist, allowing the calculations presented here to be reasonably realistic. The experience we have gained in the present work should make it possible for a subsequent survey of energy and mass dependence trends to be carried out.

In this paper we also explore the use of a "J-weighted S matrix" to encapsulate the spin-independent aspects of the channel coupling effects in a simple diagonal S matrix S_l that depends only upon the orbital angular momentum l. One reason for doing this is that $S \rightarrow V$ inversion is still unachieved for projectiles with spin greater than 1, and yet there are many projectiles, such as ^{7}Li, for which it would be interesting to derive at least the central parts of the DPP from realistic CRC calculations. The extent to which these can be derived from a "J-weighted S matrix" for spin-1 projectiles will provide an indication of whether this should also be possible for projectiles with greater spin; it also makes it possible to analyze the effects of channel coupling, in a simple way, by using near-far analysis.

[*]keeley@fuw.edu.pl
[†]Permanent address: Department of Nuclear Reactions, The Andrzej Sołtan Institute for Nuclear Studies, Hoża 69, PL-00681, Warsaw, Poland.
[‡]r.mackintosh@open.ac.uk

The plan of this paper is as follows: In Sec. II we present an outline of relevant features of deuteron scattering; Sec. III briefly reviews terminology associated with IP inversion; Sec. IV specifies the particular CRC calculation; Sec. V describes the weighted-spin calculations; Sec. VI presents the full calculations containing a representation of spin and leading to the generation of tensor interactions; Sec. VII presents an analysis of specific contributions to the DPP; and Sec. VIII presents our general conclusions.

II. BRIEF REVIEW OF DEUTERON SCATTERING

To establish the notation, we briefly review the scattering of a spin-1 projectile from a spin-0 target. This is significantly more complex than that of a spin-$\frac{1}{2}$ particle since there are five independent observables that depend on the scattering angle instead of two and there are five possible kinds of interaction potential: three kinds of tensor interaction as well as the central and spin-orbit interactions. Moreover, even elastic scattering requires, in general, a coupled channel calculation. A general account of the scattering of spin-1 projectiles can be found, for example, in Satchler's book [5], but we set down a few relevant points to establish our notation.

For spin-1 particles scattering from a spin-0 nucleus, Satchler [6] showed on the basis of symmetry considerations that there are three possible types of tensor interaction. Of these, only that designated T_R will be considered here, and it is the only one for which inversion is currently possible. (The T_L interaction is thought to be small, and the T_P interaction is hard to handle and in any case its effect is difficult to distinguish from that of T_R; see also Ref. [4].) The T_R interaction has the form

$$T_R V_R(r) \equiv [(\mathbf{s}\cdot\hat{\mathbf{r}})^2 - 2/3)]V_R(r), \tag{1}$$

where $\mathbf{s}$ is the spin operator for the projectile. As a result, the complete potential that we seek is of the form

$$V_{\rm cen}(r) + i\,W_{\rm cen}(r) + V_{\rm coul}(r) + 2\mathbf{l}\cdot\mathbf{s}(V_{\rm so} + i\,W_{\rm so}) + (V_R + i\,W_R)T_R, \tag{2}$$

where $V_{\rm coul}(r)$ is the usual spherical, uniform-charge Coulomb potential. The spin-orbit potentials $V_{\rm so}$ and $W_{\rm so}$ presented throughout this paper are defined in such a way that they will be half the magnitude of those defined according to the usual convention [5] for spin-1 projectiles.

For particular values of the conserved quantities J and π, respectively the total angular momentum and the parity, two values of orbital angular momentum, $l = J-1$ and $J+1$, are coupled by a tensor interaction T_R, whenever $\pi = (-1)^{J+1}$. The S matrix $S^J_{l'l} = S^J_{ll'}$ is defined by the asymptotic form corresponding to total angular momentum J and incident orbital angular momentum l:

$$\psi^J_{l'l}(k,r) \to \delta_{l'l} I_{l'}(kr) - S^J_{l'l} O_{l'}(kr). \tag{3}$$

Here, $I_l(r)$ and $O_l(r)$ are the incoming and outgoing asymptotic Coulomb radial wave functions, often written $H_l(r)^*$ and $H_l(r)$ as in Satchler [5], namely,

$$I_l(kr) = G_l(kr) - i\,F_l(kr), \quad O_l(kr) = G_l(kr) + i\,F_l(kr),$$

where F_l and G_l are regular and irregular Coulomb wave functions, respectively.

There are five angular dependent observables for spin-1 projectiles: the differential cross section, the vector analyzing power $i\langle T_{11}\rangle$, and the three tensor analyzing powers $\langle T_{20}\rangle$, $\langle T_{21}\rangle$, and $\langle T_{22}\rangle$, which are defined in Ref. [5]. We shall also refer to the diagonal matrix elements of the tensor operator T_R as shown in Table I.

TABLE I. The diagonal matrix elements of the tensor operator T_R.

	$l = J-1$	$l = J$	$l = J+1$
$\langle Jl\|T_R\|Jl\rangle$	$-\frac{1}{3}\frac{J-1}{2J+1}$	$\frac{1}{3}$	$-\frac{1}{3}\frac{J+2}{2J+1}$

III. ITERATIVE-PERTURBATIVE INVERSION TERMINOLOGY

The iterative-perturbative (IP) inversion technique for deriving a potential from an S matrix (or from phase shifts) is fully described in Ref. [7] and its specific implementation for spin-1 projectiles in Ref. [4]. We here briefly mention items of IP terminology that will be employed later. The IP method begins the iterative procedure from a *starting reference potential*, SRP, and expands the potential in terms of an *inversion basis*. The difference between the original S matrix to be inverted and the actual S matrix calculated from the derived potential is expressed in terms of a *phase shift distance* denoted σ, defined by

$$\sigma^2 = \sum_k \left|S^t_k - S^c_k\right|^2, \tag{4}$$

where the superscripts "t" and "c" on the S matrix indicate the target (the S matrix to be inverted) and the S matrix calculated from the potential at the current state of the iterative procedure. The sum is over all $S^J_{ll'}$, with index k labeling each combination of J, l, and l'. It is standard procedure, when one applies IP inversion, to compare potentials found with different choices of the SRP and inversion basis, noting how the potential depends (or not) upon the choice of these; this is an important means of monitoring the uniqueness of the derived potentials.

IV. CRC CALCULATIONS FOR $d + {}^{40}$Ca

In this section we present CRC calculations for the $d + {}^{40}$Ca system at an incident deuteron energy of 52 MeV. In these calculations, the incoming deuteron is coupled to mass-3 channels as specified in the following. The elastic scattering data were taken from Ermer *et al.* [8] and the (d,t) data from Doll *et al.* [9]. Data for the ^{40}Ca$(d,{}^3$He$)^{39}$K reaction were also obtained by Doll *et al.* and although they give spectroscopic factors obtained from a DWBA analysis of these data no angular distributions are presented. Obtaining the best possible description of these data helps to ensure that the calculations are realistic. All calculations were performed with the code FRESCO [3] and included the complex remnant term and nonorthogonality correction.

Together with the (d,t) and $(d,{}^3\mathrm{He})$ transfers modeled by using standard CRC with nonorthogonality corrections and remnant terms, coupling to deuteron breakup in the entrance partition was included by using the continuum discretized coupled channels (CDCC) formalism, as described in Ref. [10]. Following Ref. [10], we included both the S and D components of the deuteron ground state. Quadrupole coupling between these components, equivalent to ground-state reorientation, was included in all the calculations presented here unless explicitly stated otherwise. The neutron and proton plus ^{40}Ca optical potentials required as input to the Watanabe-type folding potentials employed in the CDCC calculation were taken from the global parametrization of Koning and Delaroche [11]. The real and imaginary depths were adjusted to obtain the best description of the elastic scattering data by the full CDCC + CRC calculation including the (d,t) and $(d,{}^3\mathrm{He})$ transfer couplings, renormalization of the real and imaginary well depths by factors of 1.0 and 0.7, respectively, giving optimum agreement.

The $d+n$ and $d+p$ form factors for the (d,t) and $(d,{}^3\mathrm{He})$ transfers were taken from Eiró and Thompson [12]. The spectroscopic amplitudes for the dominant $\ell=0$ terms of both form factors were set to $\sqrt{2}$, following Eiró and Thompson. The spectroscopic amplitudes for the small $\ell=2$ components were adjusted to give the same D_0 values as Eiró and Thompson, where D_0 is defined as

$$D_0 = \sqrt{4\pi}\int (V\psi)_0(r) r^2 dr \tag{5}$$

and $(V\psi)_0(r)$ refers to the sum of the contributions from the S and D waves:

$$(V\psi)_0(r) = V_{00}(r)\psi_0(r) + V_{02}(r)\psi_2(r). \tag{6}$$

This procedure yields the spectroscopic amplitudes for S and D components of the (d,t) and $(d,{}^3\mathrm{He})$ overlaps given in Table II.

TABLE II. Spectroscopic amplitudes for the S and D components of the (d,t) and $(d,{}^3\mathrm{He})$ overlaps. The corresponding binding potential wells were of Woods-Saxon form with parameters taken from Eiró and Thompson [12].

Overlap	S component	D component
(d,t)	1.4142	−0.1762
$(d,{}^3\mathrm{He})$	1.4142	−0.1480

We followed Doll *et al.* [9] in using the same optical model potential for both the (d,t) and $(d,{}^3\mathrm{He})$ channels, the parameters being taken from Ref. [13], again following Doll *et al.* [9]. The $p+{}^{39}$K and $n+{}^{39}$Ca binding potential wells were of Woods-Saxon form with parameters again taken from Doll *et al.* [9]. As we are interested here in the coupling effect of the (d,t) and $(d,{}^3\mathrm{He})$ pickup channels on the elastic scattering rather than spectroscopy, we somewhat arbitrarily omitted all states in ^{39}Ca and ^{39}K having spectroscopic factors less than 0.20 in the work of Doll *et al.* [9] to keep the calculation within tractable limits while retaining the bulk of the transfer strength. We found that to describe the $^{40}\mathrm{Ca}(d,t)$ data of Doll *et al.* [9] we had to reduce the spectroscopic factors obtained from their DWBA analysis by a factor of 1.8. As no data for the $(d,{}^3\mathrm{He})$ pickup are presented in Ref. [9] we also reduced the spectroscopic factors for transfers to states in ^{39}K given therein by the same factor. This discrepancy in spectroscopic factors is probably linked to the choice of normalization used in the zero-range DWBA calculations of Ref. [9] and our choice of (d,t) and $(d,{}^3\mathrm{He})$ overlap form factors. It is impossible to say which is more realistic without an extensive analysis of a large number of data sets, but in the context of this work it is sufficient that we reproduce the magnitude of the transfer cross sections.

The full calculation is compared to the data in Figs. 1 and 2. We also give the results of the no-coupling calculation and a calculation including only the deuteron breakup for the

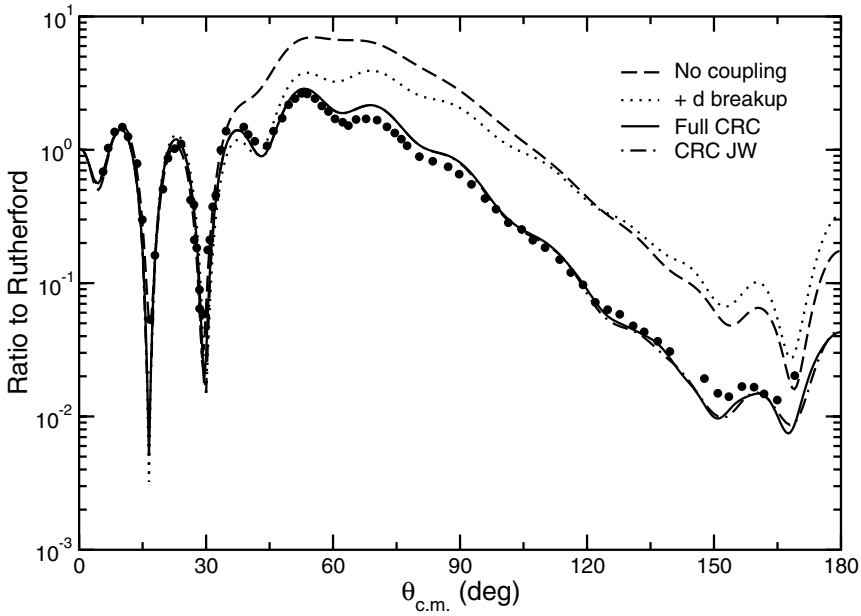

FIG. 1. Data for the $^{40}\mathrm{Ca}(d,d)$ elastic scattering [8] compared with calculations including no coupling (dashed curve), deuteron breakup only (dotted curve), and deuteron breakup plus (d,t) and $(d,{}^3\mathrm{He})$ pickup (solid curve). The dot-dashed curve gives the result for the J-weighted S matrix from the full CRC calculation (see Sec. V).

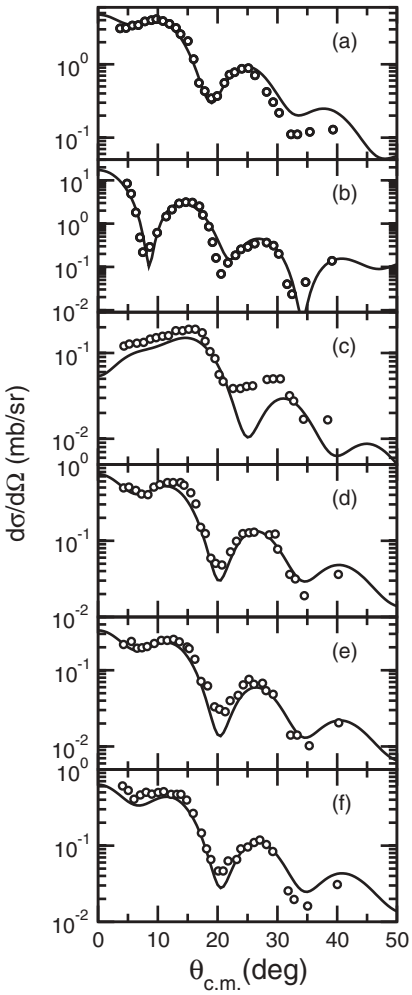

FIG. 2. Data for the ^{40}Ca$(d, t)^{39}$Ca neutron pickup reaction to the (a) 0.0-MeV $3/2^+$, (b) 2.47-MeV $1/2^+$, (c) 2.79-MeV $7/2^-$, (d) 5.13-MeV $5/2^+$, (e) 5.49-MeV $5/2^+$, and (f) 6.16-MeV $5/2^+$ states of ^{39}Ca compared to the full CDCC + CRC calculation.

elastic scattering in Fig. 1. The description of the available data is excellent. We note that there is negligible effect on the elastic scattering for angles $\theta_{\text{c.m.}} < 35^\circ$ resulting from either deuteron breakup or single nucleon pickup. Single nucleon pickup coupling becomes significant for angles greater than about 50° and is the dominant coupling effect for angles greater than about 70°.

We also carried out a calculation in which five stripping channels were included together with the pickup. The channels included were for stripping to those states in ^{41}Ca for which spectroscopic factors of 0.20 or greater were obtained in the ^{40}Ca$(d, p)^{41}$Ca study of Uozumi *et al.* [14]. Spectroscopic factors for the ^{40}Ca:^{41}Ca overlaps, $n + ^{40}$Ca binding potentials and $p + ^{41}$Ca optical potentials were all taken from Ref. [14]. Considerations of computing time made it impossible to refit parameters with these channels included. To facilitate a discussion of these and calculations with various other channels excluded, Fig. 3 represents all the various couplings considered in this paper. Notice that there is coupling between the breakup channels and the stripping channels, but not between the breakup and pickup channels, a fact that will turn out to be significant.

V. AVERAGING OVER TOTAL ANGULAR MOMENTA

We now define a "J-weighted" S matrix and then explain how we apply it. For the case of deuterons scattering from a spin-0 target, we have seen that the S matrix can be written as $S^J_{ll'}$, where J is the total conserved angular momentum quantum number. We define, for this case,

$$\bar{S}_l = \frac{\sum_J (2J+1) S^J_{ll}}{\sum_J (2J+1)}, \tag{7}$$

where the sums are over all values of J that link to l, either $l \pm 1$ or just l according to the parity. In this definition, the off-diagonal terms $S^J_{ll'}$ for $l \neq l'$ are ignored. For spin-$\frac{3}{2}$ projectiles such as ^{7}Li, where off-diagonal terms for each J exist for both parities, the same definition could be applied with the sum being over $J - \frac{3}{2}$ and $J + \frac{1}{2}$ or over $J - \frac{1}{2}$ and $J + \frac{3}{2}$ according to the parity.

We shall apply the quantity $\bar{S}_l$ in two ways: (i) in a near-far analysis [15] with the particular aim of deriving some indication of the effects of channel coupling and (ii) to apply $\bar{S}_l \rightarrow V(r)$ inversion to establish the effect of channel coupling on the central potential. The need for this latter might be questioned in view of the fact that for spin-1 we can in fact invert $S^J_{ll'}$, which leads to a potential that contains spin-orbit and tensor interactions. However, inversion for projectiles

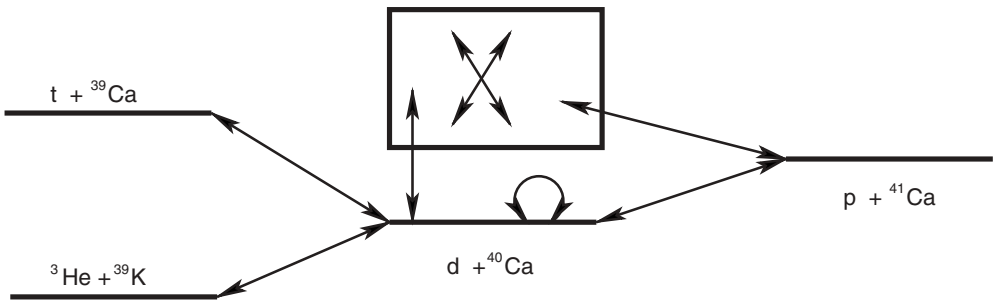

FIG. 3. The full coupling scheme of the CRC calculations; note that for clarity a single channel only is represented in each transfer partition. The box containing the crossed double-headed arrows represents the n-p continuum of the deuteron and couplings to and between the various continuum bins. The coupling loop on the $d + ^{40}$Ca entrance channel represents the deuteron ground state reorientation coupling.

such as ^{7}Li with spin > 1 is not yet possible, and it is of interest to extract at least the central potential DPP from CRC calculations in which a full representation of the projectile spin is included. Comparison of the results of $\bar{S}_l \rightarrow V(r)$ inversion and the inversion of the full $S^J_{ll'}$ should provide some measure of the general validity of the inversion of the J-weighted S matrix as a means of establishing the central components of the potential for cases where coupled channel inversion is not practicable. Even for the case of spin-1 projectiles, where the inversion is limited to the determination of T_R, the potential found by inverting $\bar{S}_l$ would be a useful comparison.

In Fig. 1, the barely discernible dot-dashed curve presents the elastic scattering differential cross section evaluated by using the J-weighted S matrix. In the present case, where there is no spin-dependent interaction, the J-weighted bare differential cross section must be identical to that shown in the dashed line.

A. Near-far decomposition for elastic scattering with channel coupling

The near-far decomposition of the angular distribution as originally introduced by Fuller [15] provides an immediate measure of the impact of the coupled reaction channels upon the elastic scattering. In Fig. 4 the angular distributions are presented in conventional rather than logarithmic form for easier comparison with the other figures in this paper, at the cost of certain insights as shown by Fuller. It can be seen that the near-side component is actually increased in magnitude by channel coupling for angles less than about 80°. However, the far-side component exceeds the near-side term beyond about 15° and, beyond the Fraunhofer region (i.e., beyond about 35°–40°), the far-side term is completely dominant. It is clear from Fig. 4 that the effect of the coupled reaction channels is a reduction in the far-side component by almost an order of magnitude between 40° and 169°, a very substantial effect.

B. Calculation of the DPP

We apply $S_l \rightarrow V(r)$ inversion [7] to the J-weighted S matrix as just defined. Figure 5 compares the bare potential and two inverted potentials, Pot1 and Pot2. These differ in that, for Pot2, the iterative inversion produced σ values that were one-tenth those of Pot1 (see Sec. III), resulting in small

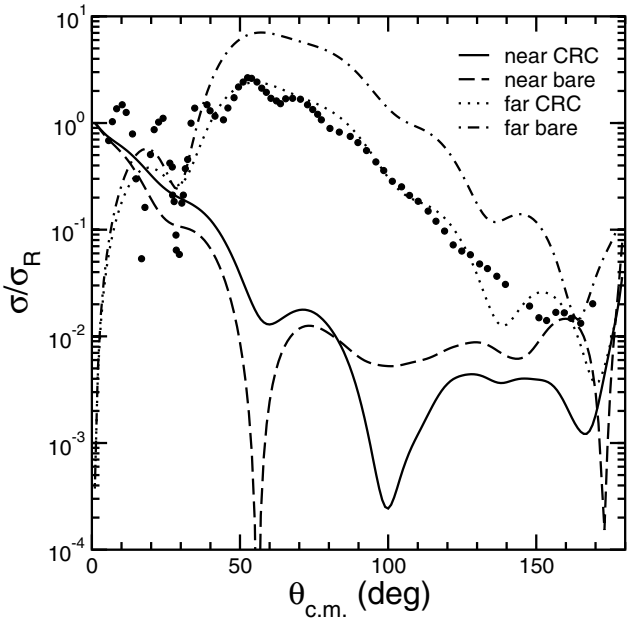

FIG. 4. Near and far differential cross sections calculated for the CRC and bare J-weighted S matrices. The solid line is for CRC-near; the dashes for bare-near; the dots for CRC-far; and the dot-dashes for bare-far. The experimental data are included, and the total J-weighted CRC differential cross section is close to these, as can be seen from the dot-dashed curve in Fig. 1, omitted here for clarity.

superimposed oscillations visible especially on the smaller magnitude imaginary term. Judging the significance of these small-amplitude and short-wavelength wiggles is a subtle and not wholly resolved problem to which we shall return when we discuss the inversion of $S^J_{ll'}$.

The real potential is somewhat changed in shape and, comparing lines 1 and 2 in Table III, we find that it has a very slightly reduced volume integral J_R and rms radius $R^{\rm rms}_R$. Table III also quantifies the very conspicuous increase in magnitude of the imaginary potential, which now takes a distinctive wavy shape. This waviness is certainly not an artifact of the inversion in the way that the small wiggles seen in Pot2 might be. In this connection, comparing the properties of Pot1 and Pot2 in Table III, we see that the wiggles on Pot2 scarcely affect J_R, $R^{\rm rms}_R$, J_I, or $R^{\rm rms}_I$ and we conclude that these four characteristics are very well determined by the inversion.

TABLE III. Characteristics of the potentials found by inverting the J-weighted S matrix. "Bare" indicates the bare potential of the CRC calculations; "Pot1" and "Pot2" represent alternative inverted potentials for the CRC S matrix found by using "Bare" as the SRP; "Daehnick" represents a potential whose real part is the global deuteron potential of Daehnick *et al.* [16] and "Potd" represents the inverted potential for the CRC S matrix found by using "Daehnick" as the SRP.

Description	J_R (MeV fm^3)	$R^{\rm rms}_R$(fm)	J_I (MeV fm^3)	$R^{\rm rms}_I$ (fm)
1 Bare	402.77	4.464	79.83	5.150
2 Pot1 (Bare SRP)	391.77	4.379	120.55	5.278
3 Pot2 (Bare SRP)	391.83	4.379	120.53	5.277
4 "Daehnick" (see text)	373.16	4.279	116.19	5.250
5 Potd ("Daehnick" SRP)	391.78	4.379	120.55	5.277

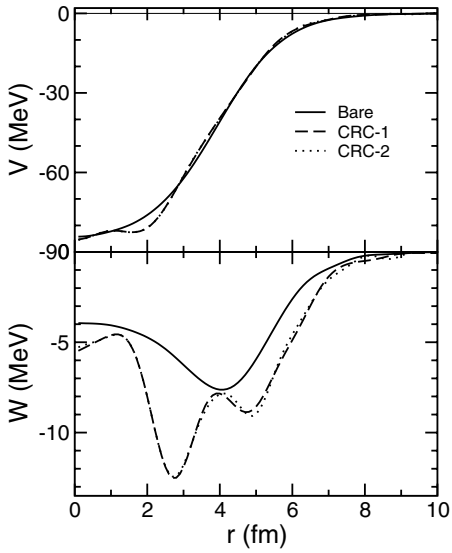

FIG. 5. Comparing the bare potential (solid line) and the two inverted potentials Pot1 (dashes) and Pot2 (dots), with the real part in the upper panel and the imaginary part below.

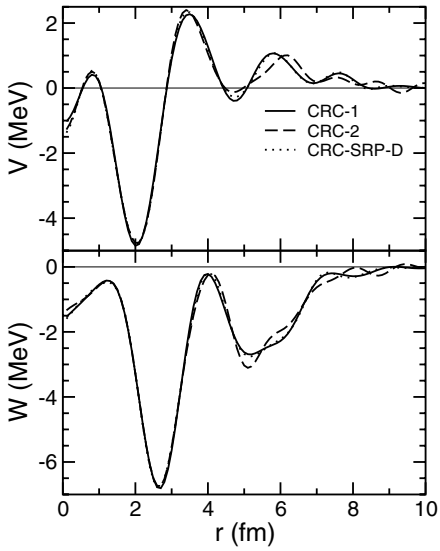

FIG. 6. The DPPs corresponding to the two inverted potentials shown in Fig. 5 (solid and dashed lines) together with the DPP determined by an independent inversion (dotted line) for which the "Daehnick" potential was the SRP. The solid and dotted lines are scarcely distinguishable.

The imaginary potential is increased in magnitude by the channel coupling at every radial point. This might be expected, but it cannot be taken for granted and neither is the fact (not illustrated) that $|S_l|$ is reduced by the channel coupling for each l. In many other cases of channel coupling (for one example see Ref. [1]), there are radial ranges over which the magnitude of the imaginary potential is reduced, as well as ranges of l over which $|S_l|$ increases, both of these features being contrary to what might be expected. In such a case, the DPP (but not always the potential itself) becomes *emissive* over certain radial regions, although the unitarity limit, $|S_l| \leqslant 1$, is never broken. These effects can be associated with the nonlocality of the underlying DPP, for which we have here determined a local representation by inversion. The l dependence and nonlocality of the underlying DPP are presumably related to the waviness of the imaginary local potential in Fig. 5. The emissive (and near-emissive found here) regions in local optical potentials were discussed in Ref. [17].

The DPP can be made explicit by subtracting the bare potential from the CRC potential shown in Fig. 5, and this is shown in Fig. 6. The imaginary part just misses becoming locally emissive at a point near 3.9 fm, and its form reinforces our belief that it is wrong to represent a DPP by multiplying a folding model potential by a normalization factor. The dotted line in Fig. 6, barely discernible from the solid line, represents the DPP derived from an independent inversion of the CRC S matrix starting from a different SRP that we refer to as the "Daehnick" potential. The real part of this SRP was the central part of the global deuteron potential of Daehnick *et al*. [16] but the imaginary part was not that of the Daehnick potential since the parameters were erroneously entered. The characteristics of this SRP are given in line 4 of Table III, and line 5 characterizes the corresponding potential inverted from the CRC S matrix. A comparison of lines 2 and 5 shows that the inverted potential is indeed independent of the SRP and that the inversion procedure has led to the unique DPP generated by the coupling to the channels specified previously.

Concerning the unusual form of the imaginary potential, we note that the model-independent phenomenology of Ermer *et al*. [8] also led to a surprising radial form, though not in agreement with the specific form found here. Their empirical imaginary central potential did have an actual emissive region, which can now be seen as plausible. Although we agree with the finding of Ermer *et al*. that the imaginary potential has a generally wavy shape, the actual "waves" are different. The origin of the disagreement is unclear, but it motivates the computationally difficult extension of these calculations to include stripping as well as pickup channels. Figures 5 and 6 illustrate a common feature of inverted potentials: There are clear oscillatory features of relatively long wavelength that may be well determined and are of dynamical origin, although a simple explanation of the particular form may not be available. There are also shorter wavelength oscillations, clearly evident in the dashed curve in Fig. 6, that appear when the iterative inversion is pushed to very low values of σ [Eq. (4)]. Although these short wavelength wiggles may well have some origin in the reaction dynamics, the results presented in this paper will generally not correspond to the lowest possible values of σ.

We conclude that, according to this J-weighted treatment, the very strong effect on the real potential of the coupling of mass-3 channels, which was found [2] with the zero-range approximation and prior to the inclusion of nonorthogonality terms, has largely disappeared, leaving an oscillatory DPP with an overall repulsive sign and having a volume integral of magnitude $\sim$11 MeV fm^3 per projectile nucleon. Channel coupling reduces the rms radius of the real part by almost 0.1 fm. The effect on the imaginary term remains substantial. We note, however, that breakup channels have also been

included, and in the discussions of the inversions involving spin that follow, we shall consider their specific contribution.

VI. FULL SPIN TREATMENT: EXTRACTION OF TENSOR INTERACTION

The full nondiagonal S matrix $S^J_{ll'}$, calculated as described in Sec. IV, was subjected to iterative-perturbative inversion leading to a potential of the form given in Eq. (2). The inversion procedure described in Ref. [4] is such that all tensor effects are represented by a T_R interaction, with possible consequences mentioned in the following.

A. Inversion of the S matrix $S^J_{ll'}$ for $d + {}^{40}$Ca

In what follows, we invert the $S^J_{ll'}$ generated with the coupling to pickup channels as well as breakup and reorientation of the deuteron (i.e., all processes except the stripping on the right-hand side of Fig. 3). The good fit in Fig. 1 corresponds to these calculations.

It is far from obvious that the full nondiagonal S matrix $S^J_{ll'}$, which arises when channel coupling is included, can be reproduced by a local, l-independent potential, including a (local, l-independent) T_R tensor term, in which the various components have a smooth radial form. In particular, we know that the inversion of an S matrix generated by an l-dependent local potential yields, in general, a potential with oscillatory features [18,19]. Hence, wavy potentials, as found for the J-weighted case, may reflect genuine dynamics corresponding to an underlying l-dependent DPP. However, the tendency for the inversion process itself to lead to potentials with spurious wiggles becomes greater when there are more components (tensor and spin-orbit) in the potential. Moreover, we cannot exclude the possibility that channel coupling might give rise to effects most naturally represented by T_P and T_L interactions. For these reasons, special care must be taken in the present case to establish what features of the potential can be extracted with assurance. This amounts to appraising the extent to which oscillatory features that might arise reflect a genuine property of the local potential that represents the effects of channel coupling rather than artifacts of the inversion procedure. To this end, various independent inversions of $S^J_{ll'}$ were undertaken by using different SRPs and inversion bases. The three SRPs used were the bare potential, the "Daehnick" potential, and the potential derived by inversion for the J-weighted case. The bare potential was itself determined by inversion of the S matrix from the uncoupled calculation.

The FRESCO [3] coupled channel calculations involve an iterative algorithm. Since numerical "noise" in the S matrix can lead to oscillations in the inverted potentials, we verified that the inverted potentials were unchanged when a more stringent convergence criterion was applied to the CRC calculations. We also verified that the final results were not undermined by a small degree of asymmetry in the CRC S matrix (i.e., $S^J_{ll'}$ is not precisely equal to $S^J_{l'l}$ for $l \neq l'$), an artifact of the CRC code FRESCO in the present application.

When we applied iterative inversion, we found that, in all cases (with different SRPs, etc.), the first few iterations yielded a good fit to all parts of the S matrix except the off-diagonal terms. At the same time, the observables were also fitted reasonably well except for T_{21}. This is consistent with the conclusion of Ref. [20] that the T_R interaction is predominantly responsible for T_{21}. At this stage of the inversion, the volume integral of the real central term is close to that found by inversion of the J-weighted S matrix.

After further iterations leading to much lower σ^2, three things happen together: (i) a substantial T_R interaction appears, (ii) T_{21} is fitted, and (iii) there is a small positive jump in the magnitude of the volume integral of the real central component. As a result of this third effect, the net effect of the channel coupling now appears, in terms of the volume integral of the real central term, to be attractive, as will be clear from the DPPs presented in the following.

Table IV encapsulates the characteristics of various potentials in terms of volume integrals as conventionally defined [5]. For comparison, line 1 contains the bare potential. Line 2 represents the J-weighted inverted potential with line 3 containing the differences between values in line 2 and line 1, characterizing the DPP calculated from the J-weighted S matrix. A quantitative representation of the final effect of channel coupling as determined by the full ($S^J_{ll'}$) inversion can be found in a comparison of lines 1 and 4 of Table IV. The difference between the J-weighted and full inversions can be seen by comparing values in lines 3 and 5. Further lines of this table are discussed later.

All components of the potential corresponding to line 4 (labeled PU; corresponding to the solid line in Fig. 1) of Table IV are given by solid lines in Fig. 7. The spin-orbit

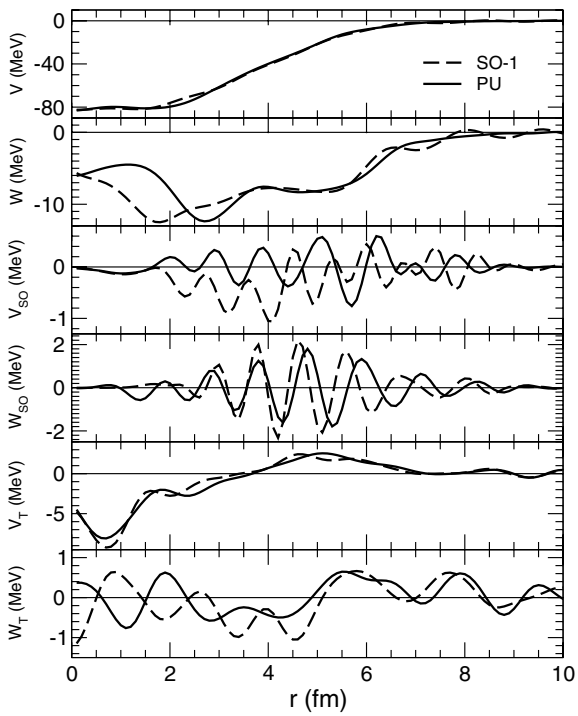

FIG. 7. The solid line represents the components of the "no-spin-orbit" potential (line 4 of Table IV) and the dashed line the "spin-orbit" potential (line 7 of Table IV). The components are, in order from the top, real central, imaginary central, real spin-orbit, imaginary spin-orbit, real tensor, and imaginary tensor.

TABLE IV. Volume integrals of potentials as specified in the text. In lines with Δ in the "Case" column, the numbers are for the DPPs found by subtracting from the line above the values in line 1; in lines with $\bar{\Delta}$, the values in line 6 have been subtracted. All quantities are in units of MeV fm^3. The columns headed CR and CI refer to the real central and imaginary central potentials, respectively. The dashes in the SOR and SOI columns (real and imaginary spin-orbit) are quantities that are very small in magnitude. The columns labeled TRR and TRI are for the real and imaginary T_R components. The line numbers in the first column are referred to in the text. In the "Case" column, PU indicates CRC including pickup, STR indicates stripping, and SO-1 and SO-2 are separate inversions of those CRC calculations in which a spin-orbit interaction was included in the bare potential.

	Case	CR	CI	SOR	SOI	TRR	TRI
1	Bare	402.77	79.83	0	0	0	0
2	J-weighted	391.77	120.55	0	0	0	0
3	Δ	−11.0	40.72	0	0	0	0
4	PU	406.38	124.01	–	–	−20.26	−4.98
5	Δ	3.61	44.18	–	–	−20.26	−4.98
6	Bare-SO	402.76	78.82	3.33	–	0	0
7	SO-1	409.74	123.10	3.10	–	−19.80	−3.26
8	$\bar{\Delta}$	6.97	43.27	0.23	–	−19.80	−3.26
9	SO-2	409.98	123.50	3.12	–	−19.99	−3.22
10	$\bar{\Delta}$	7.21	43.76	0.21	–	−19.99	−3.22
11	PU + STR	405.71	131.25	–	–	−18.70	−5.64
12	Δ	2.94	51.42	–	–	−18.70	−5.64
13	STR	414.90	112.90	–	–	−13.91	−7.72
14	Δ	12.13	33.07	–	–	−13.91	−7.72

terms, shown in the third and fourth panels of this figure, are highly oscillatory although small in magnitude and average to zero, having very small volume integrals (c.f. Sec. VI B; recall that the bare spin-orbit potential was zero in this case). The general form of the real T_R tensor potential, shown in a typical inversion as a solid line in the fifth panel in Fig. 7, is attractive for r less than about 4 fm and repulsive for r greater than about 4 fm. This general feature is well established on the basis of many inversions with different inversion bases, SRPs, etc. The fact that the repulsive region is beyond 4 fm explains why the net effect in terms of volume integral is negative, as expressed by the values in the TRR column of Table IV. The imaginary tensor term, being smaller in magnitude, is more obscured by superimposed oscillations, but there is also a clear tendency, reflected in the volume integral and rms radius, for it to be negative for r less than about 5 fm and positive further out.

The fact that J_R for the real central potential is systematically slightly greater for the full coupled channel inversions than it is for the J-weighted inversion (and Δ for J_R, line 5, for the real DPP is slightly positive rather than negative as it is in line 3) appears to be linked to the properties of the T_R interaction. From the expressions at the end of Sec. II it can be seen that we can define an l-weighted tensor force factor

$$\sum_l (2l+1)\langle Jl|T_R|Jl\rangle = -\frac{2}{2J+1}. \tag{8}$$

Thus, a negative tensor interaction also contributes an effect equivalent to a positive central interaction. It is for this reason that the volume integral of the real central potential increases somewhat at that stage in the iterative inversion process when the substantial T_R interaction appears. At the same stage in the iterative process, the rms radius of the real central potential jumps from ∼4.38 to ∼4.48 fm, as expected from the fact that the tensor interaction changes sign at ∼4 fm to become repulsive at larger radii. Similar effects, although less marked, occur with the imaginary term, too. This interplay between the central and tensor interactions implies, through the J-dependence in Eq. (8), some degree of waviness in the l-independent central potential, and probably the tensor interaction, that we extract. The oscillatory features that are evident on the small components of the potential can be understood in terms of the previously mentioned fact that strongly l-dependent potentials, whether parity dependent or having other forms of l dependence, can be represented by l-independent potentials having oscillatory or other nonregular shapes [18,19].

In Fig. 8, we compare the central components of the DPPs found in Sec. V B for the J-weighted inversion and for inversion of $S^J_{l'l}$. The real parts differ from each other in a manner that is exactly consistent with our discussion centering around Eq. (8). For example, they are very close at around 4 fm, the radius where the real tensor interaction switches from attraction to repulsion; at this radius the difference between the two curves changes sign. The increase in rms radius that was found for the J-weighted S matrix becomes in the full case a very small decrease (less than 0.01 fm). This change between J-weighted and full inversions appears to be consistent with the upper panel of Fig. 8. The imaginary parts of the DPPs are very close, but that derived from $S^J_{l'l}$ becomes slightly emissive at a point near 4 fm.

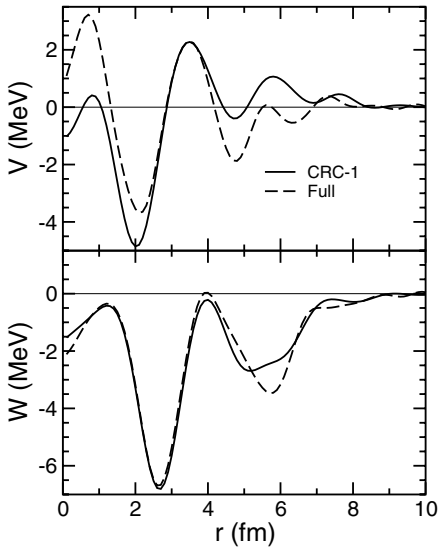

FIG. 8. Comparing the central DPPs for the J-weighted inversion (solid line) and the full inversion (dashed line); the real part is above and the imaginary part is below.

In summary, the present calculations reveal the following general properties of the l-independent, local DPP (see also line 5 of Table IV):

(i) Although the real central component of the DPP has a small volume integral, indicating marginally increased overall attraction, this term is not negligible point by point.
(ii) The imaginary central part of the DPP is substantial and generally absorptive, although the strong oscillatory character includes a small excursion into emissivity.
(iii) The real and imaginary spin-orbit components are oscillatory, but both have virtually zero volume integrals. The amplitude of the oscillations is small compared to the magnitude of the central terms.
(iv) A consistent pattern emerges for the tensor force: At the nuclear center there is attraction and absorption; at the nuclear surface there is repulsion and emission. The oscillations on the imaginary part, but not the real part, are *not* very small compared to their magnitude; however, the volume integrals of both parts appear to be well determined.

B. Inclusion of spin-orbit interaction in the deuteron potential

In the calculations described thus far, a spin-orbit interaction was omitted from the bare deuteron potential. The general importance of this interaction in deuteron scattering was explored in Ref. [21]. It was not computationally feasible to refit the elastic scattering data with a search over all the parameters, including those for the spin-orbit term, in a full CRC calculation that included all the pickup and other channels. However, we can exploit the approximate linearity of the nuclear scattering system (the basis of the IP inversion algorithm [7]) to verify that our general conclusions concerning the DPP are not affected by this omission. To do this, we simply added the spin-orbit interaction from the Daehnick global potential to the bare potential and did a single CRC calculation that included all the pickup and breakup channels, without refitting parameters. The resulting S-matrix elements $S^J_{ll'}$ were then inverted so that the DPPs could be compared with those found previously. The resulting potentials are presented as the dashed lines in Fig. 7. Line 6 of Table IV gives the characteristics of the bare potential, determined by inversion of $S^J_{ll'}$ for an uncoupled calculation with the spin-orbit term included. Lines 7 and 9 give the volume integrals for two inversions, with quite different SRPs, of the CRC $S^J_{ll'}$ and lines 8 and 10 give the corresponding increments. It can be seen that the volume integrals of the DPPs are well determined and quite similar to the values calculated with no spin-orbit interaction in the deuteron potential, the difference, $\sim$3.5 MeV fm^3, being greatest for the real central component.

We conclude that, in terms of volume integrals, the absence of the spin-orbit interaction in most of the calculations has not substantially undermined the results. However, in spite of the almost identical volume integral, the shape of the imaginary central potential did change, as seen in the dashed line in the second panel of Fig. 7. The real spin-orbit term in the third panel of this figure oscillates about the smooth shape of the spin-orbit term in the bare potential. A comparison of the entries in column SOR of lines 6, 7, and 9 of Table IV shows that the volume integral is close to that of the bare potential. It follows, therefore, that in this case the channel coupling has had essentially zero net effect on the spin-orbit potential apart from the superimposed oscillations. These oscillations resisted all efforts to eliminate them, and they may be an l-independent representation of a weak l-dependent spin-orbit DPP. We conclude that, to facilitate a comparison with the calculations described in Sec. VI A, it is reasonable to omit a spin-orbit potential from the deuteron channel potential for the purposes of the investigations to be described in the next section.

VII. UNDERSTANDING THE DPP

Two questions naturally arise: First, because the DPP presented here has contributions from deuteron breakup and reorientation as well as pickup, what are the individual contributions of these processes to the central and tensor terms? Second, what contributions would be made by processes that have been omitted, in particular, stripping? We now describe a series of calculations in which particular reaction channels were added or removed to answer such questions. In every case the parameters of the bare potential were fixed at those employed in the previous (no-spin-orbit) calculations, with no effort being made to refit differential cross section data.

A. The contribution of the stripping channels

Historically, the effect of stripping on elastic scattering was considered before the effect of pickup (see Refs. [22] and [23]). This may have been inspired by the large stripping cross section originally attributed to the weak binding of the

deuteron. However, the pickup vertex is actually stronger than the stripping vertex although the pickup cross sections are often reduced by the absorption of the outgoing particle, a consequence of momentum matching. It is now understood that the effect of a reaction channel on elastic scattering is not necessarily larger for reactions with larger cross sections, but the effects of stripping certainly deserve study. The complexity of a CRC calculation that includes both pickup and stripping processes precludes the possibility of fitting the elastic scattering with a search on the parameters for the bare potential, as was done for the pickup case.

We added five stripping channels, as specified in Sec. IV, to the deuteron pickup, breakup, and reorientation channels. As can be seen from Fig. 3, in the case of stripping there is coupling between the stripping and breakup channels, and this will be relevant in what follows. The inverted potential was characterized by the values given in lines 11 and 12 of Table IV. The Δ in line 12, characterizing the DPP, again refers to the subtraction of the bare potential values in line 1. One feature is expected: There is an appreciable increase in the central imaginary potential, $\Delta = 51.42$ MeV fm^3 as compared with 44.18 MeV fm^3 without the stripping (line 5). However, comparing lines 5 and 12 we find that the magnitudes of some of the other DPP components decrease. To get a handle on this, we inverted the CRC $S^J_{ll'}$ calculated with stripping included, *but without the pickup coupling*, with results shown in lines 13 and 14. These were initially very surprising. There is no direct coupling between the pickup and stripping channels, and it is well known that the DPPs arising from channels that are not mutually coupled should add. This should certainly be true of the underlying nonlocal and l-dependent DPPs, and it has been shown to be explicitly true for local DPPs determined by inversion (see, e.g., Ref. [24]). It is clear that the DPP components for the case with pickup plus stripping (line 12) are much smaller in magnitude than the sum of such components for pickup (line 5) and stripping (line 14) separately. The answer, of course, is that all of these calculations included the processes in the central part of Fig. 3 and that there was coupling between the *stripping* and *breakup* channels. This led us to investigate the role of the deuteron breakup and deuteron reorientation in the generation of the DPPs.

B. The roles of deuteron breakup and reorientation

To achieve some understanding of the various contributions to the DPP, we inverted $S^J_{ll'}$ for a series of different cases: (i) deuteron reorientation only, (ii) deuteron breakup plus reorientation, (iii) stripping with breakup and reorientation, (iv) pickup with no breakup or reorientation, (v) stripping with no breakup or reorientation, (vi) stripping with no breakup but with reorientation, and (vii) stripping to three lumped states and no breakup, but with reorientation. The "three lumped states" of case (vii) have the same overall pickup strength as the larger number of weaker states included in all other stripping calculations, so that the DPPs for cases (vi) and (vii) should be very close to the same if the system is linear and the inversion is reliable (a necessary though not sufficient condition, unfortunately).

TABLE V. Volume integrals of DPPs calculated from inverted potentials for various cases. The values were determined by inversion except in those cases where they were obtained by addition or subtraction, as in line 3 where the results were arrived at by subtracting the values in line 1 from those in line 2. The convention that volume integrals are positive for attractive potentials is used. In this table, REOR indicates that reorientation is included, BU signifies breakup, PU signifies pickup, and STR signifies stripping.

	Case	CR	CI	TRR	TRI
1	REOR	12.32	1.58	−17.04	−2.29
2	REOR + BU	14.21	28.45	−15.45	−4.98
3	L2 − L1 (i.e., BU)	1.89	26.87	1.59	−2.69
4	PU+ REOR +BU	3.61	44.18	−20.26	−4.98
5	L4 − L2 (i.e., PU)	−10.60	15.19	−4.81	−0.12
6	L4 − L3 (i.e., PU + REOR)	1.72	17.31	−21.85	−2.29
7	PU + REOR	−0.32	16.92	−24.25	−1.7
8	STR (No BU; No REOR)	−7.1	7.3	2.1	−2.6
9	L1 + L8 (STR + REOR)	5.22	8.9	−14.9	−4.89
10	STR + REOR	5.03	8.47	−14.19	−4.34
11	STR (3 states) + REOR	5.03	8.47	−14.18	−4.38
12	PU	−13.13	16.66	−6.49	−0.62
13	L1 + L12 (i.e., PU + REOR)	−0.81	18.24	−23.53	−2.91

Together, these calculations allow us to identify which processes contribute to the DPP, and also to verify that the DPPs originating in channels that are not coupled together do indeed add linearly. The coupling between the stripping and breakup channels means that the stripping and breakup DPPs are not additive. We shall not present detailed results of these calculations but collect in Table V volume integrals of selected DPPs. In each case these were calculated from the volume integrals calculated from the inverted potentials by subtracting the values in line 1 of Table IV. This table also includes values found by subtracting different DPPs: For example, "L2 − L1" indicates that the values in line 3 are the result of subtracting the values in line 1 from those in line 2. The volume integrals of all spin-orbit terms are very small and are not included.

From line 1, corresponding to DPPs for the case when only the reorientation terms are included, we conclude that the main source of the tensor interaction T_R is the deuteron reorientation process. There is also a real central DPP; this is related to the effect noted in Sec. VI A that the T_R interaction does make a net contribution to the central potential. Line 2 of the table shows that the addition of coupling to breakup channels markedly increases the absorptive DPP but has lesser effects on the other terms.

Since reorientation and breakup are not mutually coupled, the subtracted values in line 3 represent the effect of breakup alone. This is predominantly absorptive at this energy with a very small net attractive effect as measured by the volume integral. However, breakup induces a significant change in radial form: The rms radius of the real central potential for the case of reorientation only was 4.525 fm, whereas that for the case with both reorientation and breakup was only 4.424 fm. Comparing these two potentials (not shown) reveals that

coupling to breakup channels induces repulsion in the surface and attraction in the nuclear interior. This radial form of the breakup DPP is consistent with the effect found long ago [25]. In circumstances where the surface is dominant, the effect will appear as repulsion in spite of the net attraction noted here.

The contribution of the coupling of pickup channels is represented by line 5, in which the values in line 2 are subtracted from those in line 4, (line 5 of Table IV) representing the combined effect of pickup, breakup, and reorientation. It can be seen that the pickup channels generate an overall repulsive and absorptive component. Although the radial form of the real part is significantly changed, the fractional change to the volume integral is not large. There is, however, a significant contribution to the absorption and an increase in the strength of the tensor interaction.

It is interesting to see the additivity of the contributions in action. By subtracting line 3 (breakup as calculated by subtraction) from line 4, we should get the effect of pickup coupling plus reorientation. Line 6 presents these subtracted values and these agree qualitatively with the values in line 7 that were found by direct inversion of the S matrix for a coupled channel calculation involving just pickup and reorientation.

Another illustration of the additivity of DPPs arising from reaction channels that are not mutually coupled comes from lines 8, 9, and 10 of the table. Line 8 presents the characteristics, found by inversion, of the DPP arising from stripping alone; line 9 adds the values in line 1 to these and line 10 give the values from direct inversion of the S matrix from a calculation in which stripping and reorientation are included. The agreement between the values in lines 9 and 10 is satisfying and indicates that the inversion procedure is giving consistent values. Note that the somewhat worse agreement between lines 6 and 7 may be related to the fact that the subtracted values in line 6 are themselves obtained by subtraction. We see from line 8 that, in terms of volume integrals, the effect of stripping is remarkably small. Line 11 presents the stripping effect for the case with three lumped channels replacing the five with the same overall strength. It is almost identical to line 10; apart from showing, once more, that channels that are not mutually coupled have an additive effect, it is of practical interest in reducing the number of channels required for the CRC calculation.

We conclude that the volume integrals derived by applying inversion to coupled reaction channel and breakup calculations reveal a consistent picture and that the general procedure employed here for determining the local and l-independent representation of the dynamic polarization potentials, DPPs, that correspond to reaction channels, is robust. Further confirmation comes from the evaluation of the combined effect of pickup and reorientation by a third route. Direct evaluation by inversion of the pickup contribution with no breakup or deuteron reorientation leads to the values in line 12, which are qualitatively consistent with the values determined by subtraction in line 5. Adding these to the values in line 1 gives the values in line 13, which can be compared with the values in lines 6 and 7.

Altogether, we have achieved a consistent picture of the contributions of particular reaction channels to the various terms in the deuteron optical potential for 52-MeV deuterons scattering from ^{40}Ca, including, for the first time, the tensor interaction T_R.

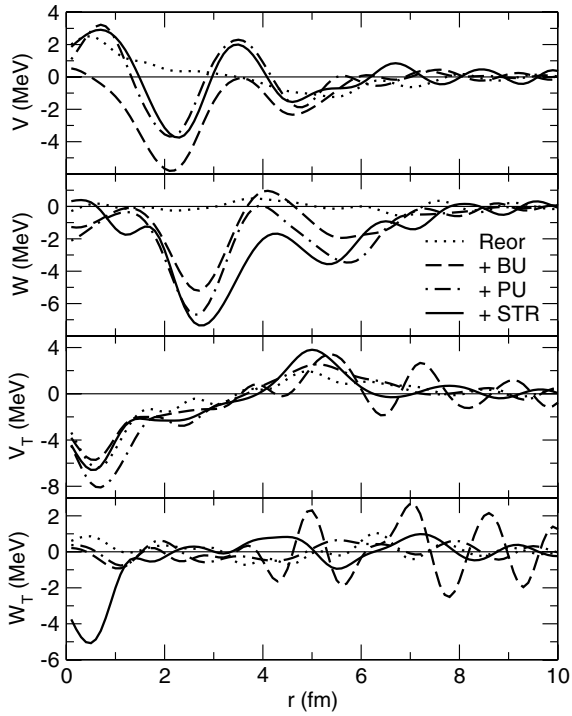

FIG. 9. Dynamic polarization potentials generated by four sets of reaction channels. From the top the DPP components are real central, imaginary central, real T_R, and imaginary T_R. Dotted lines show reorientation; dashed lines show breakup added; dot-dashed lines show pickup further added; and solid lines show all (i.e., reorientation, breakup, pickup, and stripping).

Figure 8, referred to earlier, shows the real and imaginary central DPPs for the case in which the reorientation, breakup, and pickup channels were included but gives no sense of how the different processes contribute to the radial forms. In Fig. 9 we therefore present the buildup of the central and tensor DPPs, starting with the deuteron reorientation process and the successive addition of deuteron breakup, pickup, and stripping. One can see, for example, that stripping, which was not included in Fig. 8, makes a remarkably small change to the real central term although it does contribute to the absorption, consistent with lines 4 and 11 of Table IV. The shape of the real T_R that was discussed around Eq. (8) (i.e., attractive for r less than about 4 fm and repulsive for larger r) is evident. The spin-orbit terms (not shown) are all small, oscillating about zero, consistent with their very small volume integrals.

VIII. CONCLUSIONS

The calculations we have described hardly begin to touch the wealth of phenomena associated with the coupling between deuteron channels and other channels that can be connected by direct reactions. All effects arising from the identity of

particles and exchange processes have been ignored. However, we have shown that there is no limit to what could be discovered concerning the local, l-independent representation of nucleus-nucleus interactions by linking S matrix to potential inversion to any future reaction calculations.

The present work constitutes an exacting test of the IP inversion method. As explained in Ref. [7], the instability problems that afflict formal inversion procedures can be obviated by the use of alternative bases, the control of iteration limits, etc., as we have discussed in this paper.

A. Understanding nucleus-nucleus interactions

Folding models derived from nuclear densities and based on local density models necessarily miss a range of interesting phenomena related to the specific nature of the interacting nuclei. Such models cannot be expected to represent the range of l-dependent and nonlocal effects suggested by the Feshbach formalism [26]. We also know that l-dependent and nonlocal potentials can be represented by S-matrix-equivalent potentials exhibiting wavy features. Moreover, where precise, wide angular range, elastic scattering data are fitted by supplementing folding models with additive components determined by model-independent searches, the added components are often found to have wavy features. Moreover, wavy features have long been found on potentials derived from model-independent fits to data, independent of folding models; one of many examples is Ref. [8]. It is all too easy to dismiss such fits (e.g., "how many parameters are needed to fit an elephant?") but there is surely an argument for taking the full information content of nucleus-nucleus elastic scattering data as seriously as has been done for many years with electron-nucleus scattering data. It might now become possible to make the connection between empirically derived wavy potentials and the dynamics of nucleus-nucleus potentials. The work presented here suggests, in principle at least, how this might be done.

We would put as much emphasis on the general method presented here, which demonstrably produces consistent potentials corresponding to specific reaction processes, as on the specific results of the reaction channels actually included. The coupled reaction channel calculations employed in this work were not, and could not be, comprehensive in the sense of including all reaction channels in a rigorous way and inevitably there are other possible choices of parameters. Nevertheless, the general features of the DPPs generated by a range of reaction channels have been found. The inversion procedure is, we would say, ready and waiting to be applied to S matrices produced by any future reaction calculations. It has, for possibly the first time, found the T_R tensor force, for spin-1 particles, generated by reaction processes.

A specific question addressed by this work is the following: Where inversion leading to a tensor force is impossible, does a J-weighted "spinless" inversion have any validity as a means of determining the central potentials? For example, no one to our knowledge has come close to achieving inversion for spin-$\frac{3}{2}$ particles, not least because of the forbidding diversity of possible tensor interactions. Figure 8 suggests that, indeed, the qualitative features of the central DPP can be extracted by such means, but if there is a substantial real tensor effect, it might be expected to modify the detailed results.

The coupled channel plus inversion procedure has a disadvantage compared to the direct Green function approach of Coulter and Satchler [27], for example: It fails to make explicit the nature of the l dependence and nonlocality of the DPP. However, it does have two advantages: It directly yields a local l-independent potential that can be compared with phenomenological potentials and it is straightforward within the coupled channel procedure to include all couplings between excited channels, as well as monitor the reaction cross sections.

B. Specific implications for deuteron-nucleus interactions

In Ref. [2] it was claimed that coupling to mass-3 channels generated very large contributions to the deuteron optical potential and the real part in particular. Here we have shown that much of the effect goes away with the inclusion of finite-range and nonorthogonality effects. Nevertheless, there is a contribution to the real as well as imaginary central potential although the real part of the DPP has a rather small volume integral, being positive and negative over different radial regions. It may well become possible to make a connection between specific features of the derived DPP and features found in phenomenological potentials. Moreover, there does remain a substantial imaginary DPP that can certainly be ascribed to pickup; this is much larger in magnitude than the absorptive DPP that is due to stripping. This imaginary part, too, exhibits wavy features that are characteristic of local potentials that represent intrinsically nonlocal and/or l-dependent Feshbach [26] terms. Thus, the form of the DPP, especially the imaginary part, appears to indicate that the pickup channels contribute in a way that cannot be represented by means of any local density model. We deduce, therefore, that such coupling cannot be left out of a full account of deuteron scattering, although mass-3 and mass-1 reaction channels do not, alone, solve the problem of understanding deuteron scattering. It is to be hoped that a more rigorous reaction model, containing exchange processes, for example, will become computationally feasible. If so, it will be straightforward to deduce a corresponding potential that might then be compared with potentials determined by adding a model-independent phenomenological additive term to folding model potentials.

ACKNOWLEDGMENTS

We are grateful to Professors Z. Moroz and K. Rusek for reading the manuscript and for helpful suggestions. N.K. gratefully acknowledges the receipt of a Marie Curie Actions Grant from the European Commission, Contract No. MEIF-CT-2005-010158.

[1] R. S. Mackintosh and N. Keeley, Phys. Rev. C **76**, 024601 (2007).
[2] R. S. Mackintosh, S. G. Cooper, and A. A. Ioannides, Nucl. Phys. **A472**, 85 (1987).
[3] I. J. Thompson, Comput. Phys. Rep. **7**, 167 (1988).
[4] S. G. Cooper, V. I. Kukulin, R. S. Mackintosh, and V. N. Pomerantsev, Nucl. Phys. **A677**, 187 (2000).
[5] G. R. Satchler, *Direct Nuclear Reactions* (Clarendon Press, Oxford, 1983).
[6] G. R. Satchler, Nucl. Phys. **21**, 116 (1960).
[7] V. I. Kukulin and R. S. Mackintosh, J. Phys. G: Nucl. Part. Phys. **30**, R1 (2004).
[8] M. Ermer, H. Clement, P. Grabmayr, G. J. Wagner, L. Friedrich, and E. Huttel, Phys. Lett. **B188**, 17 (1987).
[9] P. Doll, G. J. Wagner, K. T. Knopfle, and G. Mairle, Nucl. Phys. **A263**, 210 (1976).
[10] N. Keeley, N. Alamanos, and V. Lapoux, Phys. Rev. C **69**, 064604 (2004).
[11] A. J. Koning and J. P. Delaroche, Nucl. Phys. **A713**, 231 (2003).
[12] A. M. Eiró and I. J. Thompson, Phys. Rev. C **59**, 2670 (1999).
[13] P. Doll, H. Mackh, G. Mairle, and G. J. Wagner, Nucl. Phys. **A230**, 329 (1974).
[14] Y. Uozumi, N. Kikuzawa, T. Sakae, M. Matoba, K. Kinoshita, T. Sajima, H. Ijiri, N. Koori, M. Nakano, and T. Maki, Phys. Rev. C **50**, 263 (1994).
[15] R. C. Fuller, Phys. Rev. C **12**, 1561 (1975).
[16] W. W. Daehnick, J. D. Childs, and Z. Vrcelj, Phys. Rev. C **21**, 2253 (1980).
[17] R. S. Mackintosh, S. G. Cooper, and A. A. Ioannides, Nucl. Phys. **A476**, 287 (1988).
[18] S. G. Cooper and R. S. Mackintosh, Z. Phys. A **337**, 357 (1990).
[19] S. Ait-Tahar, R. S. Mackintosh, and S. G. Cooper, Nucl. Phys. **A561**, 285 (1993).
[20] D. J. Hooton and R. C. Johnson, Nucl. Phys. **A175**, 583 (1971).
[21] E. J. Stephenson, C. C. Foster, P. Schwandt, and D. A. Goldberg, Nucl. Phys. **A359**, 316 (1981).
[22] G. H. Rawitscher, Phys. Rev. **163**, 1223 (1967).
[23] T. Ohmura, B. Imanishi, M. Ichimura, and M. Kawai, Prog. Theor. Phys. **41**, 391 (1969).
[24] A. A. Ioannides and R. S. Mackintosh, Phys. Lett. **B161**, 43 (1985).
[25] A. A. Ioannides and R. S. Mackintosh, Phys. Lett. **B169**, 113 (1986).
[26] H. Feshbach, Ann. Phys. (NY) **5**, 357 (1958); **19**, 287 (1962).
[27] W. Coulter and G. R. Satchler, Nucl. Phys. **A293**, 269 (1977).